Statistical Aspects of X-Class Halo and Non-Halo Events, 1996–2014

Robert M. Wilson[1]

Abstract

Of the 166 X-class events that occurred during the interval 1996–2014, 80 had associations with halo events, 68 had no associations with halo events, and 18 occurred during LASCO data gaps. Both the duration and location of the X-class halo events proved to be statistically important parameters with respect to the geoeffectiveness of the events. Forty-four of the 80 X-class halo events occurred within 45 degrees of the Sun's central meridian and 47 of the 80 had duration ≥30 minutes, whereas only 28 of the 68 X-class non-halo events occurred within 45 degrees of the Sun's central meridian (2 events have unknown location) and 22 of the 68 had duration ≥30 minutes. Ignoring the 4 largest X-class flares ≥X4.0 during the LASCO data gaps, 17 of the remaining 20 were associated with halo events, and 14 of the 17 had at least one geomagnetically disturbed day (Ap ≥25 nT) within 1–5 days following the X-class halo event. Based on the hourly Dst index, the most geoeffective X-class halo event during the interval 1996–2014 was that of an X1.7 flare that occurred on 2001 March 29 at 0957, having an hourly Dst minimum = –387 nT. On average, the X-class halo events (80 events) were found to have a mean duration (42 minutes) slightly longer than the mean duration (29 minutes) of the X-class

[1] NASA/Marshall Space Flight Center, National Space Science Technology Center, Huntsville, Alabama 35812 USA

non-halo events (68 events) with the difference in the means being statistically important at the 1% level of significance.

Keywords: The Sun, Solar-terrestrial relations, X-class flares, Halo-CMEs

1. Introduction

X-class flares are the most energetic of solar flares, having peak fluxes in excess of 10^{-4} Wm^{-2} in the 0.1 to 0.8 nm range. Often, these X-class flares herald the occurrences of earthward-directed coronal mass ejections (CMEs) that sometimes play havoc with the Earth's magnetosphere, generating disturbances that affect satellite orbits, telecommunication and navigation systems, and electrical power grids at the Earth's surface (Allen et al. 1989, Boteler et al. 1998, Verma 2012, Wu et al. 2013, Kim et al. 2013, and Love et al. 2014).

Numerous studies previously have been performed describing specific aspects of soft x-ray flares and, in particular, their relation to energetic processes, magnetic configuration, and the occurrences of CMEs (e.g., Drake 1970, Sheeley et al. 1983, Kahler et al. 1989, Kahler 1992, Eselevich 1994, Zhongxian & Jingxiu 1994, Wilson 1996, Feldman et al. 1997, Nitta & Akiyama 1999, Zhang et al. 2001, Veronig et al. 2002, Kay et al. 2003, Wang & Zhang 2007, Gopalswamy et al. 2008, and Joshi et al. 2010). In particular, many of these studies have shown the importance of the duration of the soft x-ray flare, as well as its location on the Sun, in the occurrences of earthward-directed CMEs.

In this study, the GOES X-class flares (herein, called X-class events or XCEs) are compared with the occurrences and lack of occurrences of SOHO/LASCO halo events (HEs) to ascertain the statistics and inferred relationships that might exist between them during the

interval 1996–2014. Also examined are the statistics of geomagnetic disturbed days (i.e., Ap ≥25 nT) in relation to the occurrences of the X-class halo and non-halo events, using both Ap daily values and hourly Dst minimum values (per day) for elapsed time 1–5 days following the XCEs.

2. Results

Figure 1 displays the annual variation during the interval 1996–2014 of (a) sunspot number (SSN), (b) the number of GOES soft x-ray events (NSXRE), (c) the number of X-class events (NXCE), (d) the total number of SOHO/LASCO halo events (NHE(Total)), (e) the number of front-side halo events (NHE(FS)), and (f) the number of X-class events associated with halo events (NXCE(HE)). The data were taken from several sources, including (1) http://sidc.oma.be/silso/, (2) http://www.ngdc.noaa.gov/stp/solar/solarflares.html and (3) http://cdaw.gsfc.nasa.gov/CME_list/halo/halo.html, and span the entirety of solar cycle (SC) 23 through the rising portion of SC24.

Fig. 1 Annual variations of (a) SSN, (b) NSXRE, (c) NXCE, (d) NHE(Total), (e) NHE(FS), and (f) NXCE(HE) during the interval 1996–2014.

From Figure 1, one finds that, based on annual values, SC23 peaked in the year 2000, having SSN = 119.6 and that SC24 probably has peaked in the year 2014, having SSN = 79.0, occurring in the sixth year following its SSN minimum (=2.9 in 2008) (cf. Wilson 2011). The peak yearly NSXRE for SC23 is found to be 2,718 events in the year 2002 and perhaps to be 2,258 events in the year 2014 for SC24, following a preceding peak of 2,171 events in the year 2011. For the entire cycle, SC23 produced 23,274 soft x-ray flares, and through the year 2014, SC24 has produced 10,114 soft x-ray flares. The behavior of NXCE is observed to have been very choppy during SC23, with individual yearly peaks occurring in the years 1998 (14), 2001

(21), 2003 (20), and 2005 (17), while being much smoother on a year-to-year basis in SC24, with an observed peak (to date) of 16 events in the year 2014. The largest XCE during SC23 was that of an X28.0 event that occurred on 2003 November 4 at 1929 (start), having a duration of 37 minutes and being associated with active region (AR) 10486, a magnetically complex region (BGD) of large corrected sunspot area (630 millionths of a solar hemisphere) located at S19W83 (flare site) on the day of the event. A HE was observed for this event. The longest duration XCE during SC23 was that of an X3.8 event that occurred on 2005 January 17 at 0659 (start), having a duration of 188 minutes and being associated with AR 10720, located at N15W25 (flare site) and being a magnetically complex region (BD) and also of large corrected sunspot area (1,460 millionths of a solar hemisphere) on the day of the event. A HE was observed for this event, as well. For SC24, the largest XCE (to date) is that of an X6.9 event that occurred on 2011 August 9 at 0748 (start), having a duration of 20 minutes and being associated with AR 11263, a magnetically complex region (BGD) of large corrected sunspot area (340 millionths of a solar hemisphere), and located at N17W69 (flare site) on the day of the event. A HE was observed for this event. The longest duration XCE (to date) during SC24 is that of an X1.1 event that occurred on 2012 March 5 at 0230 (start), having a duration of 133 minutes and being associated with AR 11429, located at N16E54 (flare site) and being a magnetically complex region (BD) and also of large corrected sunspot area (770 millionths of a solar hemisphere) on the day of the event. A HE was observed for this event, as well. For the entire cycle, SC23 produced 124 XCEs and SC24 (to date) has produced 42 XCEs. For the entire interval 1996–2014, there have been 166 XCEs.

Continuing, from the SOHO/LASCO halo CME catalog (Gopalswamy et al. 2009), the peak yearly NHE(Total) measured 63 in number for the year 2001 and 84 in number for the year 2012, totaling 641 events during the interval 1996–2014, including 394 halo events in SC23 and

247 halo events (thus far) in SC24; however, it should be noted that these numbers very probably are low because of the interruptions due to the loss of observing time caused by spacecraft malfunctions during the early portion of the SOHO mission. The 641 catalogued events have been described as (1) possibly back-side events (73), (2) blimp events (82), and (3) front-side events (486). For SC23, the NHE(FS) peaked at 43 events in the year 2001 and for SC24 at 82 events in the year 2012. Overall, SC23 produced 247 NHE(FS) and SC24 (to date) has produced 239 NHE(FS). Because SC24 still has several years remaining prior to the occurrence of SC25 SSN minimum, it seems very likely that it will be the greater producer of known NHE(FS)s as compared to SC23.

For SC23, the NXCE(HE) peaked at 12 events in the year 2001, and for SC24 (to date), it has peaked at 8 events in the year 2013. For the entire cycle, SC23 produced 57 XCE(HE)s and SC24 (to date) has produced 23 XCE(HE)s, thus yielding a total of 80 XCE(HE)s for the overall interval 1996–2014. Hence, only about half (48%) of the XCEs that occurred during the interval 1996–2014 appear to be associated with SOHO/LASCO halo CME events.

Table 1 provides a summary of the yearly counts, as well as the mean and standard deviation (*sd*) of each of the parameters plotted in Figure 1, along with several other parameters. The notes below the table provide definitions for each of the parameters included in the table.

Table 1 Yearly counts, means, and standard deviations of selected parameters, 1996–2014.

From Table 1, one finds that the XCEs represent <0.5% of all SXREs (166/33,388). As noted above, only about half (48%) of the XCEs had associated HEs (80/166), 68 XCEs had no

associated HEs (41%), and 18 XCEs occurred during LDGs (11%). Of the 166 XCEs, 70 of them were located between 45 degrees east and 45 degrees west (42%) of central meridian on the Sun, 80 of them were located between 90 and 46 degrees east or 46 and 90 degrees west (48%), and 16 of them had no identified known flare site location for the X-class events (10%). Of the 80 XCEs associated with HEs, 44 of them were located between 45 degrees east and 45 degrees west (55%), and 36 of them were located between 90 and 46 degrees east or 46 and 90 degrees west (45%). Of the 166 XCEs, 92 of them had duration <30 minutes (55%), 51 of them had duration of 30–60 minutes (31%), and only 23 of them had duration >60 minutes (14%). Of the 80 XCEs associated with HEs, 33 of them had duration <30 minutes (41%), 31 of them had duration of 30–60 minutes (39%), and only 16 of them had duration >60 minutes (20%).

Tables 2 and 3, respectively, provide additional summaries of the yearly counts, means, and *sd*s for those XCEs that had no associated HEs and that occurred during LDGs. Of the 68 XCEs with no associated HEs, 22 of them were located between 45 degrees east and 45 degrees west (32%), 32 of them were located between 90 and 46 degrees east or 46 and 90 degrees west (47%), and 14 of them had no known flare site location identified for the XCEs (21%). Also, 46 of them had duration <30 minutes (68%), 13 of them had duration of 30–60 minutes (19%), and 9 of them had duration >60 minutes (13%). Of the 18 XCEs occurring during LDGs, 4 of them were located between 45 degrees east and 45 degrees west (22%), 13 of them were located between 90 and 46 degrees east or 46 and 90 degrees west (72%), and only one had no known location identified for the XCE (6%). Also, 13 of them had duration <30 minutes (72%), 4 of them had duration of 30–60 minutes (22%), and only one had duration >60 minutes (6%).

Table 2 Yearly counts, means and standard deviations of NXCE(N-HE), NXCE-N(CD), NXCE-N(NCD), NXCE-N(U), NXCE-N(<30), NXCE-N(30–60), and NXCE-N(>60).

Table 3 Yearly counts of NXCE(LDG), N(CD), N(NCD), N(U), N(<30), N(30–60), and N(>60).

Figure 2 displays the scatter plots against SSN for (a) NSXRE, (b) NXCE, (c) NHE(Total), (d) NHE(FS), (e) NXCE(HE), and (f) NXCE(N-HE), where NXCE(N-HE) refers to those XCEs not associated with a HE. In the figure, the vertical and horizontal lines are the medians, and the diagonal lines are the inferred linear regression lines. All inferred linear regressions are found to be statistically important at the 1% (or better) level of significance (i.e., the 99% or better level of confidence, *cl*). Thus, for SSN ≥56, the parameters NSXRE, NXCE, NHE(Total), NHE(FS), NXCE(HE), and NXCE(N-HE) all tend to have annual counts either equal to or higher than their respective medians (namely, ≥2,171, ≥7, ≥29, ≥40, ≥4, and ≥3), whereas for SSN, <56 all tend to have counts lower than their medians. Table 4 gives the results of the linear regression analyses against SSN, where *y* is the inferred linear regression equation, *r* is the linear coefficient of correlation, *rxr* is the coefficient of determination (a measure of the amount of variance that can be explained by the inferred linear regression), *se* is the standard error of estimate, and *cl* is the confidence level for the inferred linear regression (i.e., an indication of the statistical importance of the inferred linear regression).

Fig. 2 Scatter plots of (a) NSXRE vs. SSN, (b) NXCE vs. SSN, (c) NHE(Total) vs. SSN, (d) NHE(FS) vs. SSN, (e) NXCE(HE) vs. SSN, and (f) NXCE(N-HE) vs. SSN.

Table 4 Linear regression analysis results against SSN.

Figure 3 depicts the annual variation of (a) NXCE(HE), (b) NXCE(HE-G), (c) NXCE(HE-NG), (d) NXCE(N-HE), (e) NXCE(N-HE-G), and (f) NXCE(N-HE-NG), where NXCE(HE-G) refers to those XCE(HE)s that have at least one geomagnetically disturbed day (i.e., Ap ≥25 nT) following the XCE within 1–5 days; NXCE(HE-NG) refers to those XCE(HE)s that have no geomagnetically disturbed days following the XCE within 1–5 days; NXCE(N-HE-G) refers to those XCE(N-HE)s that are followed by at least one geomagnetically disturbed day following the XCE within 1–5 days; and NXCE(N-HE-NG) refers to those XCE(N-HE)s that have no geomagnetically disturbed days following the XCE within 1–5 days. Also given are the means and *sd*s for each of the groupings. Of the 80 XCE(HE)s that occurred during the interval 1996–2014, 54 (likely fewer) of the events are noted to have been followed within 1–5 days by at least one disturbed day (68%), indicating the possible association between the earthward-directed CME and the occurrence at Earth of a geomagnetic storm, while at least 26 of the events (likely more) had no such association (33%). (Because several of the XCE(HE)s occurred closely together in time, it sometimes is difficult to precisely identify which particular XCE(HE) is the true causative event for the following geomagnetic storm.)

Fig. 3 Annual variation of (a) NXCE(HE), (b) NXCE(HE-G), (c) NXCE(HE-NG), (d) NXCE(N-HE), (e) NXCE(N-HE-G), and (f) NXCE(N-HE-NG) during the interval 1996–2014.

Of the 68 XCE(N-HE)s, some 26 of the events had at least one geomagnetically disturbed day following the XCE within 1–5 days (38%) and 42 of the events had no geomagnetically disturbed days following the XCE within 1–5 days (62%). Additionally, there were 18 XCEs that

occurred during LDGs, of which 7 of the events were followed (39%) and 11 of them were not followed (61%) by at least one geomagnetically disturbed day within 1–5 days of the XCEs.

Table 5 gives the x-ray class (XRC) distributions for the XCE(HE)s, XCE(N-HE)s, XCE(LDG)s, and Total (i.e., the XCEs). The overwhelming majority of the events are for XRC <X4, accounting for 63 of the 80 XCE(HE)s (79%), 65 of the 68 XCE(N-HE)s (96%), 14 of the 18 XCE(LDG)s (78%), and 142 of the 166 XCEs (86%). Interesting, however, is the very close 1-to-1 association found between XCEs and HEs for XRC ≥4.0, with 17 of 20 XCEs (85%) being associated with a HE (disregarding the 4 XCE(LDG)s).

Table 5 Distributions of NXCE(HE), NXCE(N-HE), NXCE(LDG), and Total based on XRC.

Table 6 gives the duration distributions for the XCE(HE)s, XCE(N-HE)s, XCE(LDG)s and Total. For the XCE(HE)s, 44 of the 80 XCE(HE)s have duration >30 minutes (55%), while only 18 of the 68 XCE(N-HE)s and 4 of the 18 XCE(LDG)s have duration >30 minutes (26% and 22%, respectively). For all XCEs, 68 of the 166 events have duration >30 minutes (41%). Of the 68 XCEs having duration >30 minutes, 44 of them are associated with HEs (65%).

Table 6 Distributions of NXCE(HE), NXCE(N-HE), NXCE(LDG), and Total based on XCE duration.

Table 7 gives the central meridian distance (CMD) distributions for the XCE(HE)s, XCE(N-HE)s, XCE(LDG)s, and Total. Plainly, all groupings of XCEs are found to essentially

occur at all CMDs (i.e., from limb-to-limb on the Sun), with only a slight increase in XCE(HE)s within the central disk portion (44/80 or 55%) and the western hemisphere (46/80 or 58%). Still, it is noteworthy that 13 XCE(HE)s occurred on or near the eastern and western limbs (i.e., at CMD >80 degrees from Sun center; 16%).

Table 7 Distributions of NXCE(HE), NXCE(N-HE), NXCE(LDG), and Total based on XCE CMD.

Table 8 gives the active region magnetic classification (ARMC) distributions for the XCE(HE)s, XCE(N-HE)s, XCE(LDG)s and Total, based on the Mount Wilson sunspot magnetic classification scheme and taken from the extended Greenwich sunspot data listings (http://solarscience.msfc.nasa.gov/greenwch.shtml). Plainly, the overwhelming majority of the XCEs are associated with magnetically complex sunspot groups (BG, BD, and especially BGD), accounting for 130 of the 166 XCEs (78%), 70 of the 80 XCE(HE)s (88%), and 52 of the 68 XCE(N-HE)s (76%). It should be noted that the XCEs associated with simpler magnetically classified regions often are those found near the limb, and therefore, might not be properly classified magnetically (due to foreshortening).

Table 8 Distributions of NXCE(HE), NXCE(N-HE), NXCE(LDG), and Total based on ARMC.

Table 9 gives the corrected active region area (CARA) distribution (in units of millionths of a solar hemisphere) for each of the groupings XCE(HE)s, XCE(N-HE)s, XCE(LDG)s, and

Total. While XCEs can originate from ARs of generally any size, the vast majority are found to be associated with ARs of large CARA. For ARs having CARA >400 millionths of a solar hemisphere, one finds that this accounts for 109 of the 166 XCEs (66%), 56 of the 80 XCE(HE)s (70%), 47 of the 68 XCE(N-HE)s (69%), and 6 of the 18 XCE(LDG)s (33%).

Table 9 Distributions of NXCE, NXCE(HE), NXCE(N-HE), NXCE(LDG), and Total based on CARA.

Table 10 identifies the 24 largest XCEs that occurred during the interval 1996–2014, arranged in descending order from largest to smallest XRC, providing the GOES start-max-end times of the XCEs, duration (in minutes), GOES peak XRC, AR location (taken from the GOES x-ray event listings, http://www.ngdc.noaa.gov/stp/solar/solarflares.html, when available; otherwise, it was taken from http://cdaw.gsfc.nasa.gov/CME_list/halo/halo.html or http://solarscience.msfc.nasa.gov/greenwch.shtml), the active region number (ARN), ARMC, CARA, Ap daily value for 0–5 days from the XCE occurrence date, hourly Dst minimum value per day for 0–5 days from the XCE occurrence date, and comments regarding the occurrences of halo events (start time), the apparent speed (*AS*) and the computed space speed (*SS*) of the halo event, and the occurrences of LDGs. Also given are the means and *sd*s for the daily Ap and hourly Dst values and the durations of the XCEs and sunspot areas of the associated AR. The durations of the 24 largest XCEs span 12–93 minutes, averaging about 35 minutes. Nineteen of the 24 events are associated with magnetically complex ARs (79%), and the ARs responsible for the XCEs are found to span 88 degrees east to 85 degrees west, averaging about 943 millionths of a solar hemisphere in corrected sunspot area. Seventeen of the XCEs had at least one

geomagnetically disturbed day 1–5 days following the occurrence of the XCE (71%); 12 of the 17 XCE(HE)s had at least one geomagnetically disturbed day 1–5 days following the occurrence of the associated XCE (71%); 2 of the 3 XCE(N-HE)s had at least one geomagnetically disturbed day 1–5 days following the occurrence of the XCE (67%); and 3 of the 4 XCE(LDG)s had at least one geomagnetically disturbed day 1–5 days following the occurrence of the associated XCE (75%).

Table 10 Listing of the largest X-class events (XRC = X4.0 or greater), 1996–2014 (24 events).

Figures 4 and 5 show, respectively, the scatter plots of the *SS* versus the XRC and the duration (in minutes) of the XCE. The vertical, horizontal, and diagonal lines in the figures have the same meanings as before (in Figure 2). Both correlations are inferred to be statistically important (*cl* >99.5%) and suggest that when the XCE has an XRC of X2 or higher or the duration is 35 minutes or longer, the computed *SS* is at least twice as likely to be ≥1,600 km s^{-1}. Table 11 gives the results of the linear regression analyses for *SS* versus XRC and duration. A bivariate fit of *SS* against the combined effects of both XRC and duration (not shown) only slightly improves the inferred fit, having $R_{y.12} = 0.545$, $S_{y.12} = 615.883$ km s^{-1}, and an inferred regression equation of $y = 1{,}130.227 + 62x_1 + 9.434x_2$, where y is *SS*, x_1 is XRC, and x_2 is duration.

Fig. 4 Scatter plot of *SS* vs. XRC.

Fig. 5 Scatter plot of *SS* vs. duration.

Table 11 Linear regression analysis results for *SS* versus XRC and duration.

Figure 6 displays the scatter plot of *SS* versus the CMD, where negative values represent eastern AR locations and positive values represent western locations. Clearly, no inferred preferential linear association is found between *SS* and CMD (i.e., the location of the XCE(HE) on the Sun).

Fig. 6 Scatter plot of *SS* vs. CMD.

Figures 7 and 8 depict, respectively, the largest geomagnetic storm and two other large storms during the interval 1996–2014 attributable to the occurrences of XCE(HE)s. Plotted are the hourly variations of (a) the scalar magnetic field (B, in nT), (b) the Bz (GSM) component (in nT), (c) the proton density (PD, in number of protons cm^{-3}), (d) the plasma speed (PS, in km s^{-1}), and (e) the Dst (in nT); these data were taken from the OMNI website (http://omniweb.gsfc.nasa.gov/form/dx1.html). Figure 7 plots the parameters associated with the X1.7 event from AR 9393 that occurred on 2001 March 29 at 0957, having a duration of 35 minutes, CARA of 2,440 millionths of a solar hemisphere, ARMC of BGD, and flare site location of N20W19. The XCE was associated with a HE that started at 1026 and had a computed *SS* = 1,130 km s^{-1}. About 33 hours after the XCE, the PD began to increase, and about 39 hours after the XCE, both the B and Bz sharply increased, with the Bz vacillating from 25.2 nT to –40 nT to 25.8 nT to –35 nT on March 31. The CME passage at Earth lasted about one day. Initially, the Dst is observed to have been increasing towards positive values, while the PS was decreasing from about 570 to 400 km s^{-1}. However, as soon as the B and Bz increased, the

PS sharply increased, as well (from about 400 km s^{-1} to 720 km s^{-1} and then higher to about 820 km s^{-1} a day later). With the strong southward-turning of Bz (i.e., –Bz values), the value of the hourly Dst immediately decreased from about 26 nT to –387 nT on March 31 (0800), with recovery following thereafter over the next few days (cf. Russell et al. 1974, Wilson 1990, and Tsurrutani et al. 1992). Storm conditions are observed to have prevailed from about 0500 on March 31 through about 1900 on April 2. (Storm conditions are said to occur when the hourly Dst minimum <–50 nT, with the storm being described as "moderate" when the hourly Dst minimum is between –50 and –100 nT, "strong" or "intense" when the hourly Dst minimum is between –100 and –200 nT, "severe" when the hourly Dst minimum is between –200 and –350 nT, and "great" or "exceptional" when the hourly Dst minimum is <–350 nT; Loewe & Prölss 1997.)

Fig. 7 Hourly variation of (a) B, (b) Bz (GSM), (c) PD, (d) PS, and (e) Dst for the X1.7 event of 2001 March 29.

Fig. 8 Hourly variation of (a) B, (b) Bz (GSM), (c) PD, (d) PS, and (e) Dst for the X17.2 and X10.0 events of 2003 October 28 and 29, respectively.

Figure 8 shows the geoeffectiveness of two other XCEs, close together in time and both from AR 10486. The first is attributed to the X17.2 event that occurred on 2003 October 28 at 0951, having a duration of 93 minutes, CARA of 2,120 millionths of a solar hemisphere, ARMC of BGD, and flare site location of S16E08. It is associated with a HE that started at 1130 and had a computed SS = 3,128 km s^{-1}. The second is attributed to the X10.0 event that occurred from the same AR on 2003 October 29 at 2037, having a duration of 24 minutes, CARA of 2,610

millionths of a solar hemisphere, ARMC of BGD, and flare site location of S15W02. It too was associated with a HE, one that started at 2054 and had a computed $SS = 2{,}628$ km s^{-1}. Unfortunately, the solar wind data are incomplete for these two events, with only the hourly B, Bz, and Dst being known (i.e., there is a three-day interval when the hourly PD and PS data are not available). Both events appear to last about one day each (based on the behavior of B), with the first attaining an hourly Dst minimum of –353 nT on October 30 at 0000 and the second attaining an hourly Dst minimum of –383 nT on October 30 at 2200. Storm conditions are observed to have continued from about 0600 on October 29 to about 0700 on November 1.

3. Discussion and Conclusions

In terms of annual counts, the NSXRE for SC23 (1996–2007) peaked in the year 2002, some 2 years following SSN maximum, although the NSXRE is essentially flat during the 3-year interval 2000–2002, as shown in Figure 1. For SC24 (through the year 2014), the NSXRE may have peaked in the year 2014, although it is only slightly larger than the earlier peak in the year 2011, which occurred in the rising portion of the cycle, some 3 years following SSN minimum and some 3 years prior to its assumed SSN maximum. Strictly speaking, the findings of a delayed NSXRE relative to SSN maximum for SC23 and no delay for SC24 are consistent with that suggested for earlier even- and odd-numbered cycles by Wheatland & Litvinenko 2001, Temmer et al. 2003, and Yan et al. 2011.

For NXCE, similar findings are found, with NXCE peaking in the year 2001 in SC23 and possibly peaking in the year 2014 in SC24. It should be noted, however, that the yearly temporal behavior of the NXCE is much different for SC23 as compared to that of SC24. In SC23, the NXCE varies considerably from year to year, whereas in SC24, it is much smoother in appearance. For NHE(Total) and NHE(FS), the year 2012 is the most productive, numbering 84

and 82, respectively. However, it must be remembered that because interruptions plagued the SOHO spacecraft in its early years of observing the Sun, the numbers during the early years might not be reliable (i.e., they might be slightly undercounted). Perhaps surprisingly, one finds that only about half of the XCEs during the interval 1996–2014 are associated with HEs, with no associations occurring during the years 2007–2010 (i.e., during the interval 2007–2010, there were no XCEs and only 16 HE(Total)s, including 13 HE(FS)s).

Regarding the correlation between NSXRE, NXCE, NHE(Total), NHE(FS), NXCE(HE), and NXCE(N-HE) against SSN, each of the inferred linear correlations is found to be statistically significant at the 1% level of significance or better. The inferred correlation between NXSRE and SSN is the strongest, having $r = 0.875$ and $rxr = 0.766$ (meaning that nearly 77% of the variance in NSXRE can be explained by the inferred correlation against SSN). Therefore, presuming SSN <56 in the year 2015 and beyond, one anticipates fewer than 2,171 SXREs, 7 XCEs, 29 HE(Total)s, 20 HE(FS)s, 4 XCE(HE)s, and 3 XCE(N-HE)s per year during each of the remaining years of SC24.

The largest XCE during the interval 1996–2014 was that of an X28.0 flare on 2003 November 4, having duration of 37 minutes, location of S19W83, and association with a HE. While this event was associated with a HE, its geoeffectiveness, as determined by the Ap and Dst indices, was rather weak, having a daily Ap and hourly Dst minimum of only 29 and –33 nT, respectively, on elapsed time 5 days after the XCE. Indeed, the most geoeffective XCE(HE) was that of an X1.7 flare on 2001 March 3, having duration of 35 minutes, location of N20W19, and daily Ap and hourly Dst minimum of 192 and –387 nT, respectively, on elapsed time 3 days after the XCE. (A larger daily Ap = 204 nT was observed on 2003 October 29, possibly associated with the X17.2 flare that occurred on 2003 October 28.)

Thus far, the largest XCE during SC24 has been an X6.9 flare on 2011 August 9, having a duration of 20 minutes, a location of N17W69, and an association with a HE. However, as with the X28.0 flare, it was not strongly geoeffective. The most geoeffective XCE(HE) thus far in SC24 is that of an X5.4 flare, having a duration of 38 minutes, location of N17E27, and daily Ap and hourly Dst minimum values of 87 and –143 nT on elapsed time 2 days after the XCE.

Interesting is that of the 20 largest XCEs having XRC ≥4.0 (excluding the 4 XCEs that occurred during LDGs), 17 of them were associated with HEs (85%), and of the 17 XCE(HE)s, 14 were followed within 5 days by a geomagnetically disturbed day storm (82%). Only 3 of the 24 largest XCE(HE)s have occurred in SC24 (13%).

The *SS* associated with XCE(HE)s is found to be related to both the XRC and the duration of the XCE, accounting for about 30% of the variance in *SS*, based on the inferred bivariate fit. In particular, the *SS* is about twice as likely to equal or exceed 1,600 km s^{-1} when the XCE(HE) has an XRC ≥2.0 and/or duration ≥35 minutes. No statistically important relation is found between *SS* and the location of the XCE on the Sun (i.e., the CMD).

Table 12 provides a summary of the counts for various groupings of XCE, XCE(HE), and XCE(N-HE) during SC23 and SC24 (through the year 2014). Interesting is the comparison of the first 7 years of SC23 and SC24. For SC24 (the first 7 years, 2008–2014), there have been some 4,238 fewer SXREs, 30 fewer XCEs, only 3 fewer NHEs (probably indicating an undercount during SC23 due to the interruptions of observing time), 11 fewer XCE(HE)s, 9 fewer XCE(N-HE)s, 17 fewer XCE(CD)s, 16 fewer XCE(NCD)s, 19 fewer XCE (<30), 12 fewer XCE(30–60), one more XCE(>60), 17 fewer XCE(HE,CD)s, 6 more XCE(HE, NCD)s, 2 fewer XCE(HE, <30)s, 10 fewer XCE(HE, 30–60)s, one more XCE(HE, >60), 5 more XCE(N-HE, CD)s, 14

fewer XCE(N-HE, NCD)s, 10 fewer XCE(N-HE, <30)s, the same XCE(N-HE, 30–60)s, and one more XCE(N-HE, >60).

Table 12 Cyclic parametric values.

Table 13 gives the means and *sd*s of duration and CMD for different groupings of XCEs: XCE(HE), XCE(N-HE), XCE(HE-G), XCE(N-HE-G), XCE(HE-NG), and XCE(N-HE-NG). A comparison of the mean durations of the 80 XCE(HE)s and 68 XCE(N-HE)s shows that the difference in the means is statistically important at the 1% level of significance (based on the *t* statistic for independent samples; Lapin 1978). Similarly, a comparison of the mean durations of the 54 XCE(HE-G)s and the 42 XCE(N-HE-NG)s reveals an even stronger statistically important difference in the means (at the 0.5% level of significance). Hence, XCE(HE)s of longer mean duration tend to be associated with geomagnetically disturbed days in the 1–5 days after the XCE, while XCE(N-HE)s of shorter mean duration tend not to be associated with geomagnetically disturbed days in the 1–5 days after the XCE.

Table 13 Mean duration and CMD for selected groupings of XCEs.

Likewise, a comparison of the mean CMDs of the 80 XCE(HE)s and the 66 XCE(N-HE)s (there were 2 XCE(N-HE)s that had no CMD determination) shows that the difference in means is barely statistically important at the 5% level of significance. However, a comparison of the mean CMDs of the 54 XCE(HE-G)s and the 40 XCE(N-HE-NG)s shows that the difference is statistically very important at the 0.5% level of significance. Additionally, a comparison of the

mean CMDs of the 54 XCE(HE-G)s and the 26 XCE(HE-NG)s, as well as a comparison of the mean CMDs of the 54 XCE(HE-G)s and the 26 XCE(N-HE-G)s, shows that the difference is highly statistically significant at the 0.1% level of significance. Hence, XCE(HE)s that occur closer to Sun center appear to have a much greater chance of causing a magnetic storm at Earth than XCE(HE)s or XCE(N-HE)s that occur farther away from Sun center (cf. Lyons et al. 1999, Srivastava & Venkatakrishnan 2004, Moon et al. 2005, Gopalswamy et al. 2007, Zhang et al. 2007, Rawat et al. 2010, Kilcik et al. 2011, and Cid et al. 2012).

Acknowledgements

Acknowledgement is expressed for the use of (1) the annual sunspot numbers taken from the Sunspot Index and Long-term Solar Observations, Royal Observatory of Belgium, Brussels via their web page http://sidc.oma.be/silso/; (2) the solar wind OMNI data listings via the web page http://omniweb.gsfc.nasa.gov/form/dx1.html; (3) the GOES x-ray event listings via the web page http://www.ngdc.noaa.gov/stp/solar/solarflares.html; and (4) the extended Greenwich sunspot data listings maintained at NASA/Marshall Space Flight Center, Huntsville, Alabama, via the web page http://solarscience.msfc.nasa.gov/greenwch.shtml.

References

Allen, J. & Sauer, H. 1989, Eos, 70(46), 1479.

Boteler, D. H., Pirjola, R. J., & Nevanlinna, H. 1998, Adv. Space Res., 22(1), 17.

Cid, C., Cremades, H., Aran, A., et al. 2012, JGR, 117, A11102.

Drake, J. F. 1971, Solar Phys., 16(1), 152.

Feldman, U., Doschek, G. A., & Klimchuk, J. A. 1997, ApJ, 474, 511.

Gopalswamy, N., Akiyama, S., & Yashiro, S. 2008, Proc. IAU Symp. No. 257, Universal Heliophysical Processes, ed. N. Gopalswamy & D. F. Webb, 283.

Gopalswamy, N., Yashiro, S., & Akiyama, S. 2007, JGR, 112, A06112.

Gopalswamy, N., Yashiro, S., Michalek, G., et al. 2009, Earth Moon Planet, 104, 295.

Joshi, N. C., Bankoti, N. S., Pande, S., et al. 2010, New Astron., 15, 538.

Kahler, S. W. 1992, Annu. Rev. Astron. Astrophys., 30, 113.

Kahler, S. W., Sheeley Jr., N. R., & Liggett, M. 1989, ApJ, 344, 1026.

Kay, H. R. M., Harra, L. K., Matthews, S. A., Culhane, J. L., & Green, L. M. 2003, A&A, 400, 779.

Kilcik, A., Yurchyshyn, V. B., Abramenko, V., Goode, P.R., et al. 2011, ApJ, 727, 44(6 pp.)

Kim, R.-S., Gopalswamy, N., Cho, K.-S., Moon, Y.-J., & Yashiro, S. 2013, Sol. Phys., 284, 77.

Lapin, L. L. 1978, Statistics for Modern Business Decisions (2nd ed., New York, Harcourt Brace Jovanovich, Inc.)

Loewe, C. A. & Prölss, G. W. 1997, JGR, 102(A7), 14209.

Love, J. J., Rigler, E. J., Pulkkinen, A., & Balch, C. C. 2014, Eos, 95(48), 445.

Lyons, M. A., Stockton-Chalk, A. B., & Lewis, D. J. 1999, Proc. ESPM-9, Magnetic Fields and Solar Processes, 943.

Moon, Y.-J., Cho, K.-S., Dryer, M., et al. 2005, ApJ, 624, 414.

Nitta, N. & Akiyama, S. 1999, ApJ, 525, L57.

Rawat, R., Alex, S., & Lakhina, G. S. 2010, JASTP, 72, 1364.

Russell, C. T., McPherron, R. L., & Burton, R. K. 1974, JGR, 79(7), 1105.

Sheeley Jr., N. R., Howard, R. A., Koomen, M. J., & Michels, D. J. 1983, ApJ, 272, 349.

Srivastava, N. & Venkatakrishanan, P. 2004, JGR, 109, A10103.

Tsurutani, B. T. Gonzalez, W. D., Tang, F., & Lee, Y. T. 1992, Geophys. Res. Lett., 19(1), 73.

Verma, P. L. 2012, IJOPS, 1(1), 7.

Veronig, A., Temmer, M., Hanslmeier, A., Otruba, W., & Messerotti, M. 2002, A&A, 382, 1070.

Wang, Y. & Zhang, J. 2007, ApJ, 665, 1428.

Wheatland, M. S. & Litvinenko, Y. E. 2001, ApJ, 557, 332.

Wilson, R. M. 1990, JGR, 95(A1), 215.

Wilson, R. M. 1996, Planet. Space Sci., 44(5), 441.

Wilson, R. M. 2011, NASA/TP—2011–216461, 32 pp.

Wu, C.-C., Gopalswamy, N., Lepping, R. P., & Yarshiro, S. 2013, Terr. Atmos. Ocean Sci., 24(2), 233.

Yan, X. L., Deng, L. H., Qu, Z. Q., & Xu, C. L. 2011, Astrophys. Space Sci., 333, 11.

Zhang, J., Dere, K. P., Howard, R. A., Kundu, M. R., & White, S. M. 2001, ApJ, 559, 452.

Zhang, J., Richardson, I. G., Webb, D. F., et al. 2007, JGR, 112, A10102.

Zhongxian, S. & Jingxiu, W. 1994, Sol. Phys., 149, 105.

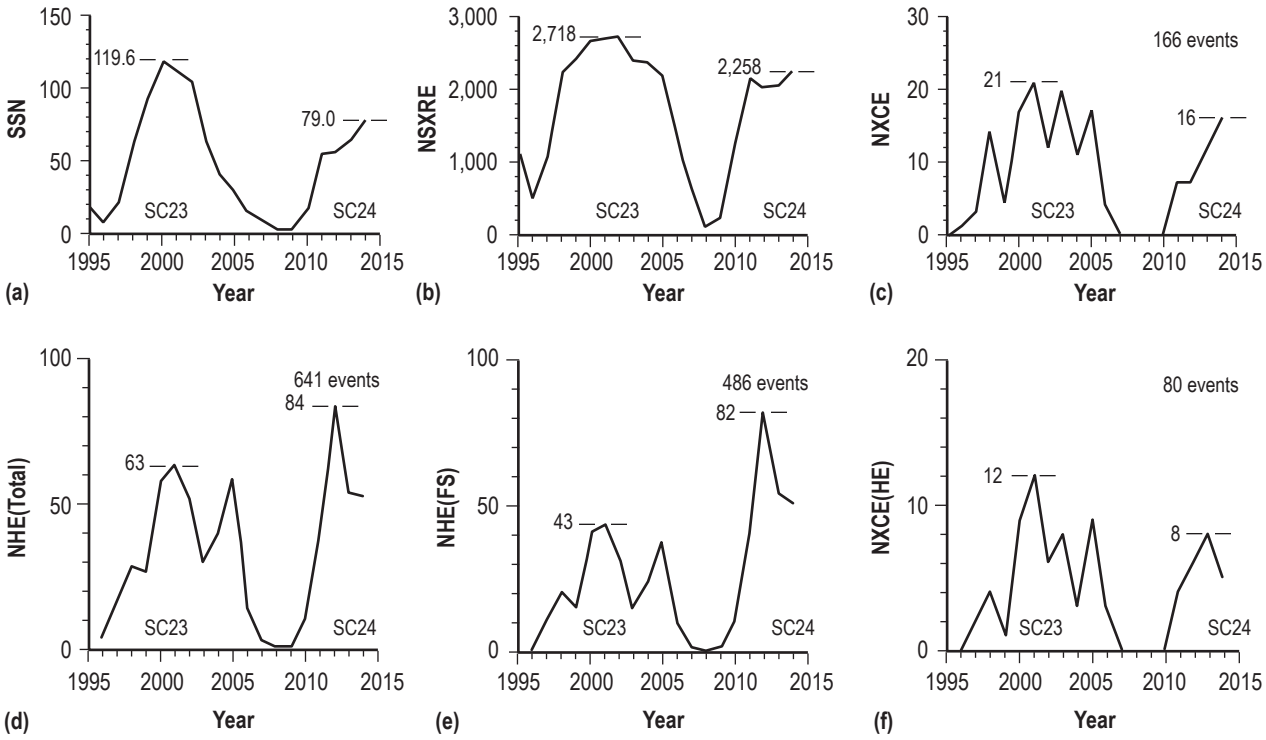
SSN
150
100
50
0
119.6
79.0
SC23
SC24
1995
2000
2005
2010
2015
Year
(a)
NSXRE
3,000
2,000
1,000
0
2,718
2,258
SC23
SC24
Year
(b)
NXCE
30
20
10
0
166 events
21
16
SC23
SC24
Year
(c)
NHE(Total)
100
50
0
641 events
84
63
SC23
SC24
Year
(d)
NHE(FS)
100
50
0
486 events
82
43
SC23
SC24
Year
(e)
NXCE(HE)
20
10
0
80 events
12
8
SC23
SC24
Year
(f)

F1_1522

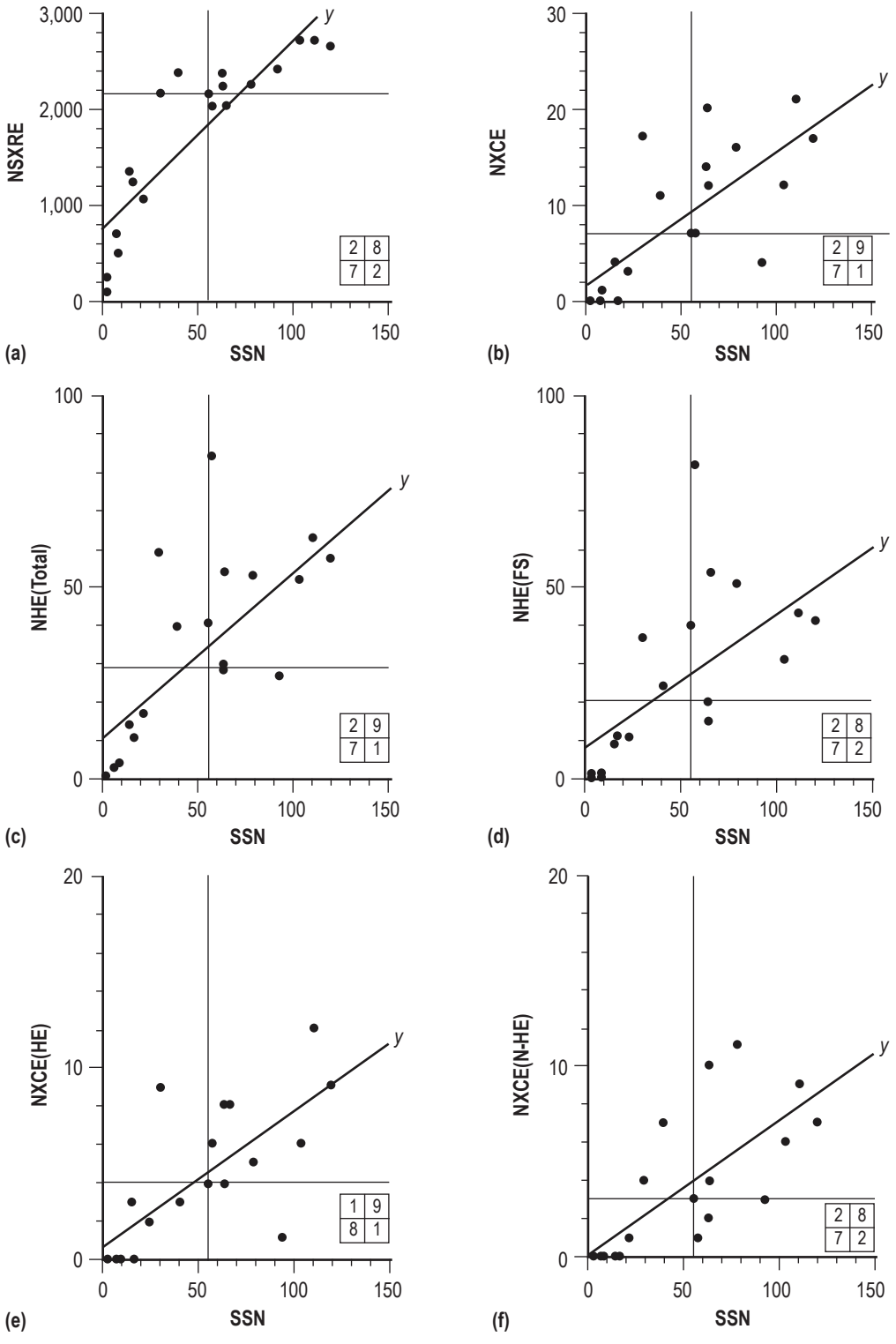
(a)
NSXRE
SSN
y
3,000
2,000
1,000
0
0
50
100
150
2 8
7 2
(b)
NXCE
SSN
y
30
20
10
0
0
50
100
150
2 9
7 1
(c)
NHE(Total)
SSN
y
100
50
0
0
50
100
150
2 9
7 1
(d)
NHE(FS)
SSN
y
100
50
0
0
50
100
150
2 8
7 2
(e)
NXCE(HE)
SSN
y
20
10
0
0
50
100
150
1 9
8 1
(f)
NXCE(N-HE)
SSN
y
20
10
0
0
50
100
150
2 8
7 2

F2_1522

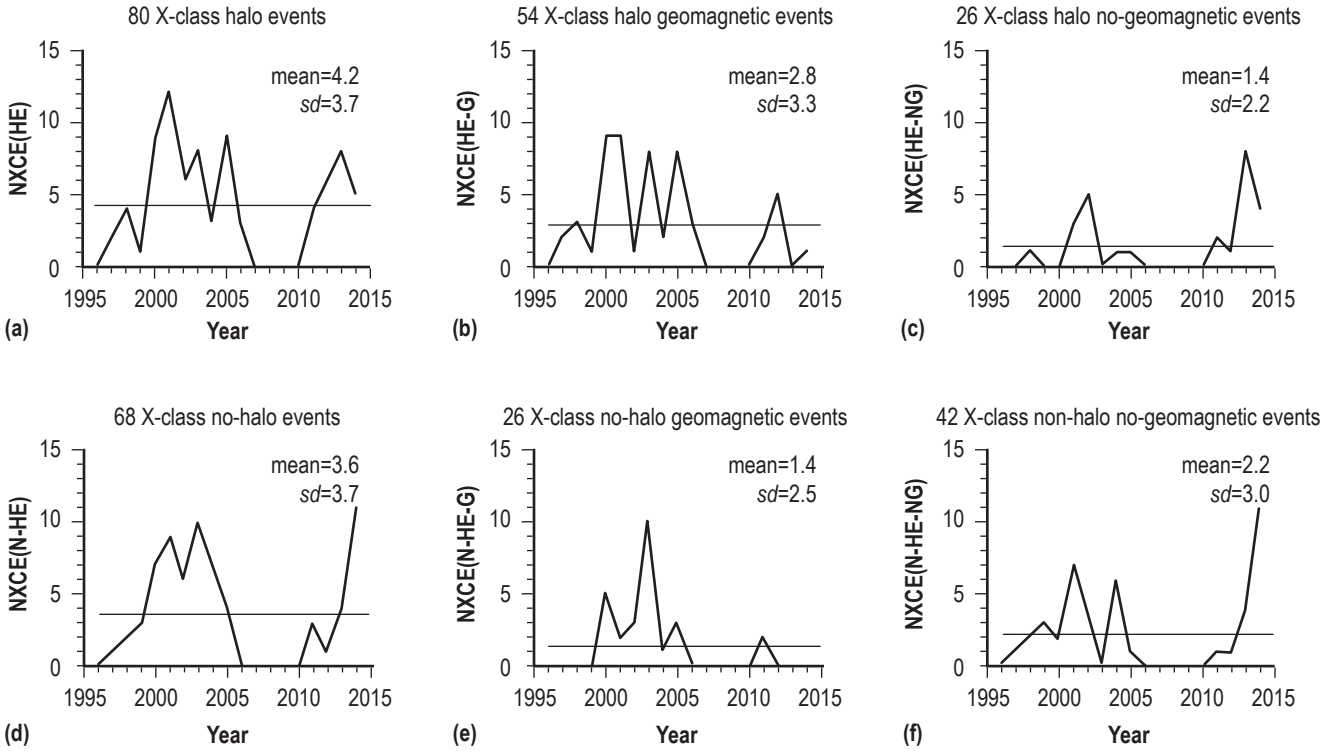
80 X-class halo events
mean=4.2
sd=3.7
NXCE(HE)
(a)
54 X-class halo geomagnetic events
mean=2.8
sd=3.3
NXCE(HE-G)
(b)
26 X-class halo no-geomagnetic events
mean=1.4
sd=2.2
NXCE(HE-NG)
(c)
68 X-class no-halo events
mean=3.6
sd=3.7
NXCE(N-HE)
(d)
26 X-class no-halo geomagnetic events
mean=1.4
sd=2.5
NXCE(N-HE-G)
(e)
42 X-class non-halo no-geomagnetic events
mean=2.2
sd=3.0
NXCE(N-HE-NG)
(f)
0
5
10
15
1995
2000
2005
2010
2015
Year

F3_1522

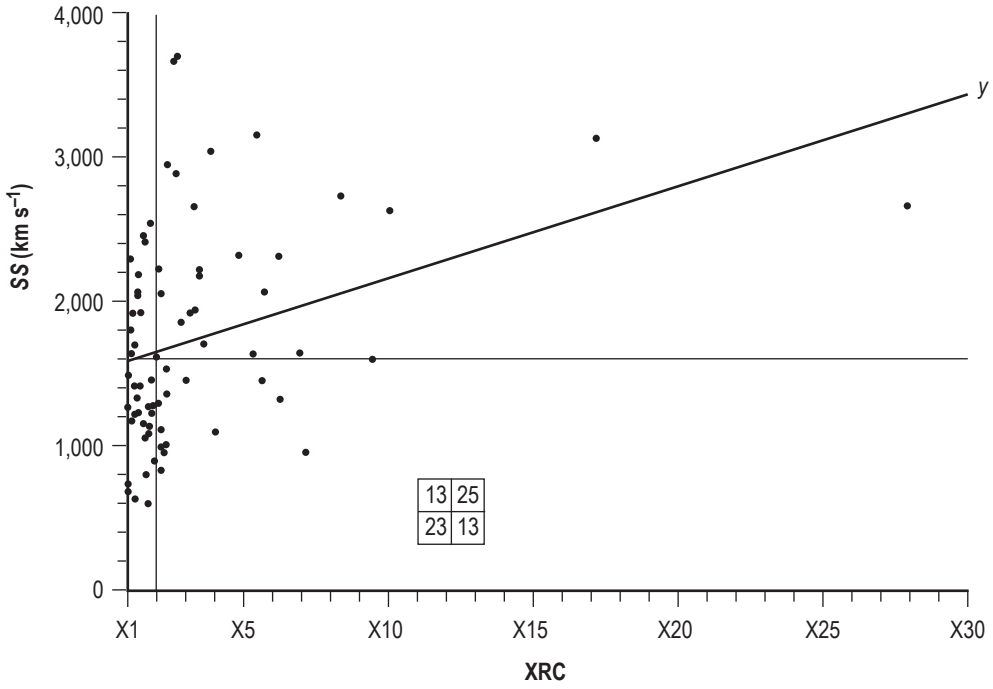
4,000
3,000
2,000
1,000
0
SS (km s−1)
y
13 25
23 13
X1
X5
X10
X15
X20
X25
X30
XRC

F4_1522

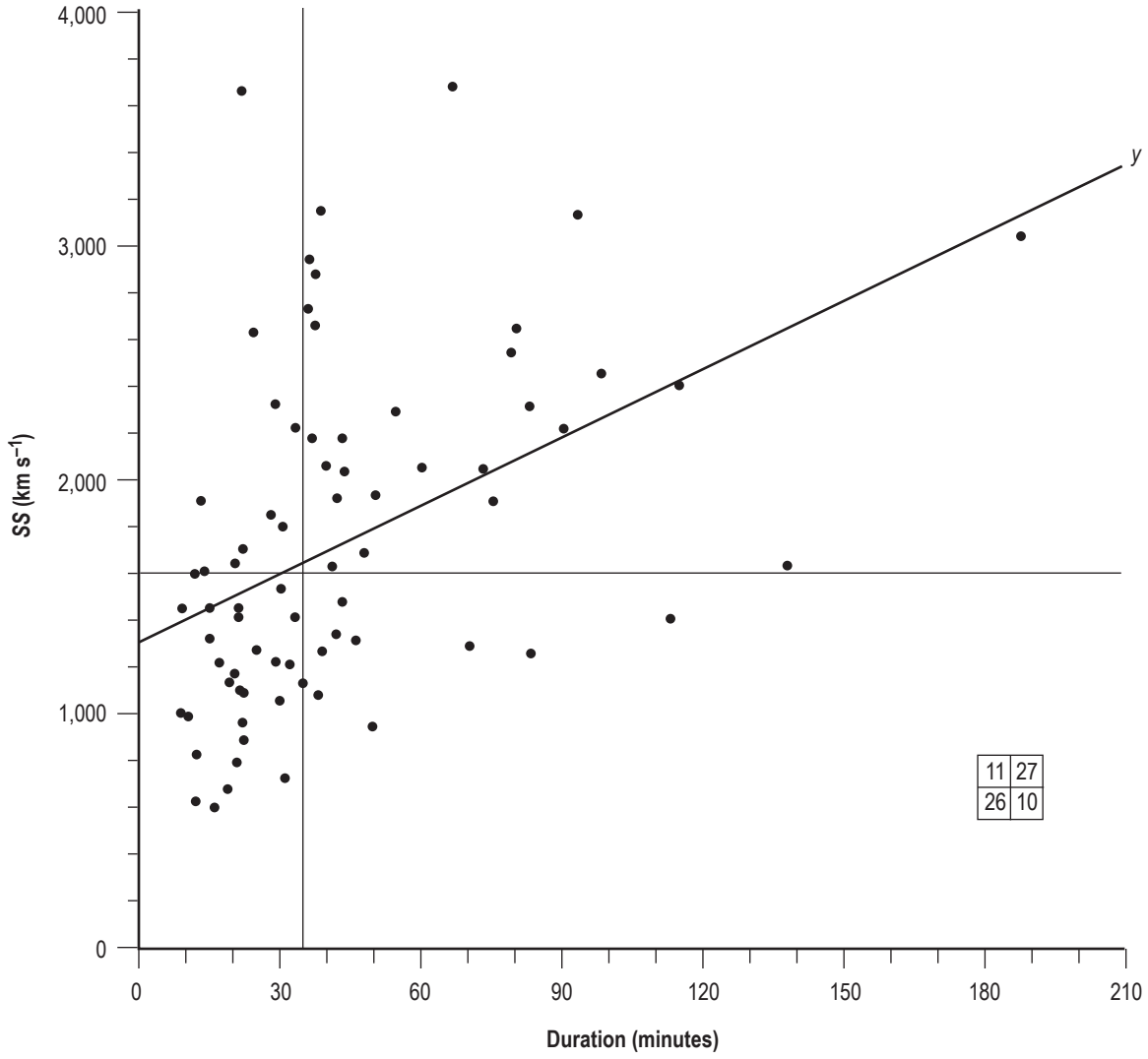
4,000
3,000
2,000
1,000
0
SS (km s^{-1})
y
11 27
26 10
0
30
60
90
120
150
180
210
Duration (minutes)

F5_1522

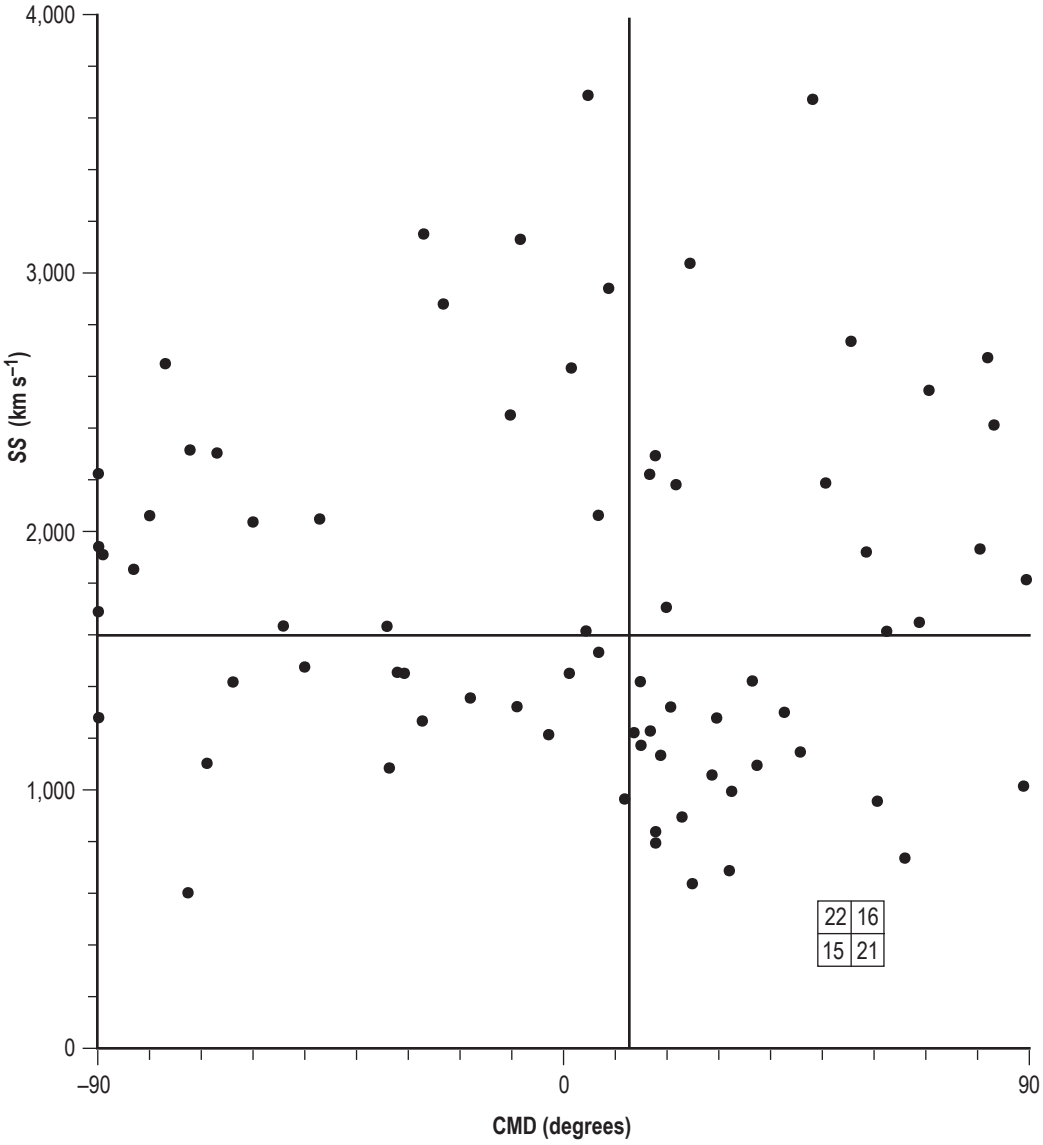

F6_1522

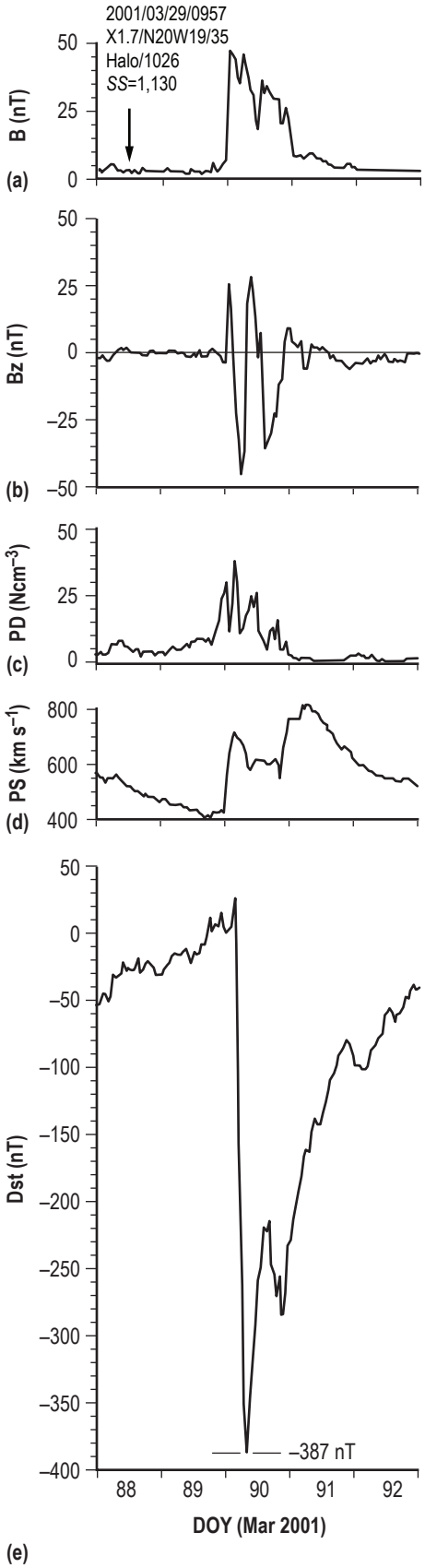
2001/03/29/0957
X1.7/N20W19/35
Halo/1026
SS=1,130
B (nT)
(a)
Bz (nT)
(b)
PD (Ncm^{-3})
(c)
PS (km s^{-1})
(d)
Dst (nT)
–387 nT
DOY (Mar 2001)
(e)

F7_1522

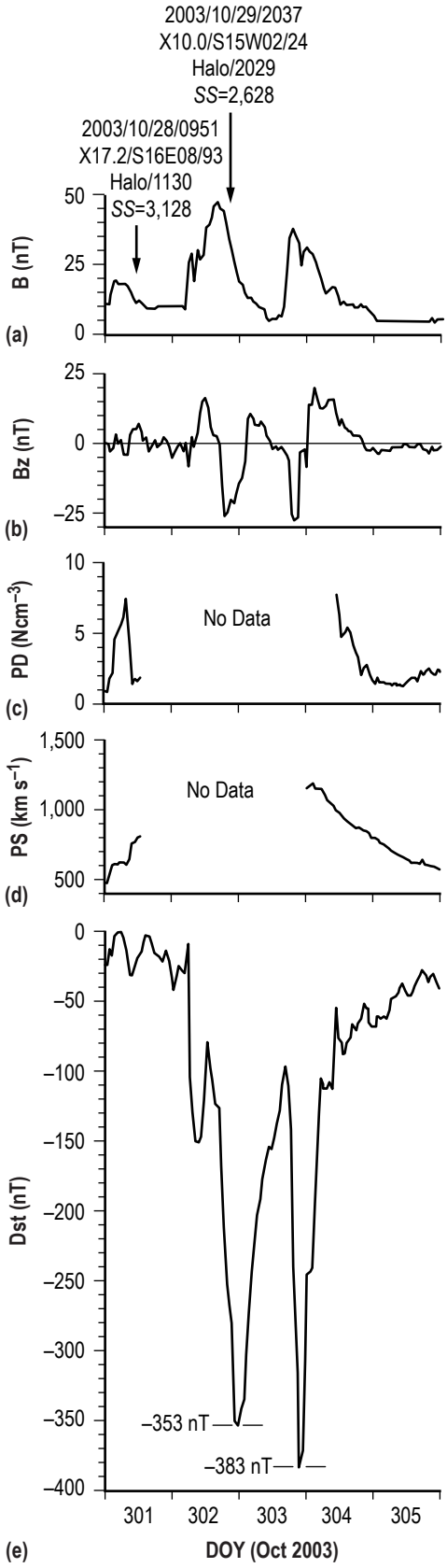
2003/10/29/2037
X10.0/S15W02/24
Halo/2029
SS=2,628
2003/10/28/0951
X17.2/S16E08/93
Halo/1130
SS=3,128
B (nT)
50
25
0
(a)
Bz (nT)
25
0
–25
(b)
PD (Ncm–3)
10
5
0
No Data
(c)
PS (km s–1)
1,500
1,000
500
No Data
(d)
Dst (nT)
0
–50
–100
–150
–200
–250
–300
–350
–400
–353 nT
–383 nT
301
302
303
304
305
DOY (Oct 2003)
(e)

F8_1522

				NHE			NXCE						NXCE(HE)		NXCE			NXCE(HE)			
Year	**SSN**	**NSXRE**	**NXCE**	**LXCE**	**Total**	**FS**	**HE**	**N-HE**	**LDG**	**CD**	**NCD**	**U**	**CD**	**NCD**	**<30**	**30–60**	**>60**	**<30**	**30–60**	**>60**	**Comment**
1996m	8.6	510	1	X2.6	4	0	0	0	1	1	0	0	0	0	0	1	0	0	0	0	SC23 SSN min
1997	21.5	1,085	3	X9.4	17	11	2	1	0	1	2	0	1	1	3	0	0	2	0	0	
1998	64.3	2,248	14	X4.9	29	20	4	2	8	3	10	1	1	3	8	5	1	1	3	0	
1999	93.3	2,424	4	X1.8	27	15	1	3	0	2	2	0	1	0	4	0	0	1	0	0	
2000M	119.6	2,661	17	X5.7	58	41	9	7	1	9	6	2	9	0	12	4	1	4	4	1	SC23 SSN max
2001	111.0	2,706	21	X20.0	63	43	12	9	0	14	4	3	11	1	7	10	4	3	7	2	
2002	104.0	2,718	12	X4.8	52	31	6	6	0	2	9	1	2	4	8	3	1	3	2	1	
2003	63.7	2,394	20	X28.0	30	15	8	10	2	9	10	1	5	3	9	8	3	4	2	2	
2004	40.4	2,369	11	X3.6	40	24	3	7	1	8	3	0	2	1	10	1	0	2	1	0	
2005	29.8	2,171	17	X17.0	59	37	9	4	4	4	10	3	3	6	6	6	5	0	4	5	
2006	15.2	1,339	4	X9.0	14	9	3	0	1	1	3	0	1	2	2	2	0	1	2	0	
2007	7.5	649	0	…	3	1	0	0	0	0	0	0	0	0	0	0	0	0	0	0	
2008m	2.9	86	0	…	1	0	0	0	0	0	0	0	0	0	0	0	0	0	0	0	SC24 SSN min
2009	3.1	256	0	…	1	1	0	0	0	0	0	0	0	0	0	0	0	0	0	0	
2010	16.5	1,255	0	…	11	11	0	0	0	0	0	0	0	0	0	0	0	0	0	0	
2011	55.7	2,171	7	X6.9	41	40	4	3	0	2	2	3	2	2	6	1	0	3	0	1	
2012	57.7	2,037	7	X5.4	84	82	6	1	0	3	3	1	3	3	3	1	3	2	1	3	
2013	64.9	2,051	12	X3.3	54	54	8	4	0	4	8	0	0	8	8	3	1	4	3	1	
2014M	79.0	2,258	16	X4.9	53	51	5	11	0	7	8	1	3	2	6	6	4	3	2	0	SC24 SSN max
Totals		33,388	166		641	486	80	68	18	70	80	16	44	36	92	51	23	33	31	16	
mean	50.5	1,757.3	8.7		33.7	25.6	4.2	3.6		3.7	4.2		2.3	1.9	4.8	2.7	1.2	1.7	1.6	0.8	
sd	38.4	868.3	7.3		24.8	22.4	3.7	3.7		3.9	3.8		3.1	2.2	3.8	3.0	1.7	1.5	1.9	1.3	

Note: SSN means sunspot number; values taken from http://sidc.oma.be/silso/
NCXE means number of X-class events
LXCE means largest X-class event
NHE means number of halo events
FS means front-side
HE means halo event
N-HE means no-halo event
LDG means LASCO Data Gap
CD means central disk (i.e., event location between 45 deg east and 45 deg west)
NCD means non-CD (i.e., event location outside 45 deg east or west)
U means the location is unknown (i.e., not given in the GOES soft x-ray event listing)
NXCE(HE) means the number of X-class events with an associated halo event
The numbers <30, 30–60, and >60 refer to the durations in minutes of the X-class events
SC means solar cycle
m means SC minimum (SC min)
M means SC maximum (SC max)
sd means standard deviation

NXCE-(N-x)							
Year	**HE**	**CD**	**NCD**	**U**	**<30**	**30–60**	**>60**
1996	0	0	0	0	0	0	0
1997	1	0	1	0	1	0	0
1998	2	1	1	0	1	0	1
1999	3	1	2	0	3	0	0
2000	7	0	5	2	7	0	0
2001	9	3	3	3	4	3	2
2002	6	0	5	1	5	1	0
2003	10	3	6	1	4	4	2
2004	7	5	2	0	7	0	0
2005	4	1	1	2	3	1	0
2006	0	0	0	0	0	0	0
2007	0	0	0	0	0	0	0
2008	0	0	0	0	0	0	0
2009	0	0	0	0	0	0	0
2010	0	0	0	0	0	0	0
2011	3	0	0	3	3	0	0
2012	1	0	0	1	1	0	0
2013	4	4	0	0	4	0	0
2014	11	4	6	1	3	4	4
Totals	68	22	32	14	46	13	9
mean	3.6	1.2	1.7	0.7	2.4	0.7	0.5
sd	3.7	1.7	2.2	1.0	2.3	1.4	1.1

Note: NXCE-(N-HE) means the number of X-class events with no associated halo event
NXCE-(N-CD) means the NXCE-(N-HE) within CD
NXCE-(N-NCD) means the NXCE-(N-HE) not within CD
NXCE-(N-U) means the NXCE-(N-HE) with no known location
NXCE-(N-<30) means the NXCE-(N-HE) with duration <30 min
NXCE-(N-30–60) means the NXCE-(N-HE) with duration 30–60 min
NXCE-(N->60) means the NXCE-(N-HE) with duration >60 min

NXCE-x							
Year	**LDG**	**CD**	**NCD**	**U**	**<30**	**30–60**	**>60**
1996	1	1	0	0	0	1	0
1997	0	0	0	0	0	0	0
1998	8	1	6	1	6	2	0
1999	0	0	0	0	0	0	0
2000	1	0	1	0	1	0	0
2001	0	0	0	0	0	0	0
2002	0	0	0	0	0	0	0
2003	2	1	1	0	1	1	0
2004	1	1	0	0	1	0	0
2005	4	0	4	0	3	0	1
2006	1	0	1	0	1	0	0
2007	0	0	0	0	0	0	0
2008	0	0	0	0	0	0	0
2009	0	0	0	0	0	0	0
2010	0	0	0	0	0	0	0
2011	0	0	0	0	0	0	0
2012	0	0	0	0	0	0	0
2013	0	0	0	0	0	0	0
2014	0	0	0	0	0	0	0
Totals	18	4	13	1	13	4	1

Association	Equation	*r*	*rxr*	*se*	*cl*
NSXRE vs. SSN	$y = 757.274 + 19.818x$	0.875	0.766	431.926	>99.9%
NXCE(HE) vs. SSN	$y = 0.748 + 0.069x$	0.753	0.567	2.682	>99.9%
NXCE vs. SSN	$y = 1.678 + 0.140x$	0.731	0.535	5.146	>99.9%
NXCE(N-HE) vs. SSN	$y = 0.051 + 0.070x$	0.722	0.521	2.643	>99.9%
NHE(Total) vs. SSN	$y = 10.286 + 0.465x$	0.719	0.517	17.701	>99.9%
NHE(FS) vs. SSN	$y = 8.146 + 0.345x$	0.592	0.350	18.592	>99%

XRC	NXCE(HE)	NXCE(N-HE)	NXCE(LDG)	Total
X1.0–1.9	39	52	7	98
X2.0–2.9	17	7	4	28
X3.0–3.9	7	6	3	16
X4.0–4.9	3		1	4
X5.0–5.9	4	1	1	6
X6.0–6.9	4			4
X7.0–7.9	1			1
X8.0–8.9	1			1
X9.0–9.9	1		1	2
X10.0–10.9	1			1
X11.0–11.9				
X12.0–12.9				
X13.0–13.9				
X14.0–14.9		1		1
X15.0–15.9				
X16.0–16.9				
X17.0–17.9	1	1		2
X18.0–18.9				
X19.0–19.9				
X20.0–20.9			1	1
X21.0–21.9				
X22.0–22.9				
X23.0–23.9				
X24.0–24.9				
X25.0–25.9				
X26.0–26.9				
X27.0–27.9				
X28.0–28.9	1			1
X29.0–29.9				
X30.0+				
Totals	80	68	18	166

Note: XRC means x-ray class

Duration	NXCE(HE)	NXCE(N-HE)	NXCE(LDG)	Total
0–10	3	12	1	16
11–20	14	23	6	43
21–30	19	13	7	39
31–40	15	6		21
41–50	10	4	3	17
51–60	4	1	1	6
61–70	2	2		4
71–80	4	3		7
81–90	3	1		4
91–100	2	2		4
101–110				
111–120	2	1		3
121–130				
131–140	1			1
141–150				
151–160				
161–170				
171–180				
181–190	1			1
Totals	80	68	18	166

CMD	NXCE(HE)	NXCE(N-HE)	NXCE(LDG)	Total
90–81E	8	3	1	12
80–71E	4	2	3	9
70–61E	3	3	3	9
60–51E	3	6	1	10
50–41E	2	7		9
40–31E	4	4		8
30–21E	3	2	1	6
20–11E	2	3		5
10–0E	5	3	1	9
0–10W	8			8
11–20W	11	4		15
21–30W	7	2	1	10
31–40W	4	5	1	10
41–50W	3	2		5
51–60W	3	5	1	9
61–70W	4	4		8
71–80W	1	4		5
81–90W	5	7	4	16
Unknown		2	1	3
Totals	80	68	18	166

Note: CMD means central meridian distance

ARMC	NXCE(HE)	NXCE(N-HE)	NXCE(LDG)	Total
Unknown	5	2	4	11
A	2	2	2	6
B	3	12	4	19
BG	13	7	2	22
BD	6	3		9
BGD	51	42	6	99
Totals	80	68	18	166

Note: ARMC means active region magnetic class and follows the Mount Wilson Magnetic Classification Scheme
A means "Alpha," a unipolar sunspot group
B means "Beta," a bipolar sunspot group
BG means "Beta-Gamma," a more complex bipolar sunspot group with no clear magnetic neutral line
BD means "Beta-Delta," a more complex bipolar sunspot group with one or more "delta" sunspots, where a "delta" sunspot is one having the umbrae of opposite polarity in a single penumbra
BGD means "Beta-Gamma-Delta," the most complex of sunspot groups having a general "beta-gamma" magnetic configuration, but containing one or more "delta" sunspots
Unknown means that the ARMC for the active region responsible for the XCE could not be determined (usually meaning that the sunspot group had traversed the limb)

CARA	NXCE(HE)	NXCE(N-HE)	NXCE(LDG)	Total
Unknown	5	2	4	11
1–100	3	4	2	9
101–200	6	7		13
201–300	5	2	2	9
301–400	5	6	4	15
401–500	12	10		22
501–600	6	4	1	11
601–700	7	5		12
701–800	7	4		11
801–900	5	4		9
901–1,000	3	2		5
1,001–1,500	10	8	5	23
1,501–2,000	2	6		8
2,001–3,000	4	4		8
Totals	80	68	18	166

Note: CARA means the corrected active region area in millionths of the solar hemisphere (i.e., it has been corrected for foreshortening). The CARA determinations were taken from http://solarscience.msfc.nasa.gov/greenwch.shtml

Date	Start	Max	End	Dur	XRC	AR Loc	ARN	ARMC	CARA	Ap (Daily)						Hourly Dst Minimum Per Day						Comment
										0	1	2	3	4	5	0	1	2	3	4	5	
2003-11-04%	1929	1950	2006	37	X28.0	S19W83	10486	BGD	630	38	6	17	8	8	29	–69	–41	–25	–20	–5	–33	H/1954, *AS*/2,657, *SS*/2,662
2001-04-02	2132	2151	2203	31	X20.0	N17W60^	9393	BGD	1,810	22	6	23	19	13	20	–101	–41	–31	–50	–31	–42	
2003-10-28%	0951	1110	1124	93	X17.2	S16E08	10486	BGD	2,120	25	204	191	116	26	18	–32	–350	–383	–307	–69	–41	H/1130, *AS*/2,459, *SS*/3,128
2005-09-07%	1717	1740	1803	46	X17.0	S11E77	10808	A	10	10	6	17	33	101	75	–33	–29	–36	–73	–139	–89	LDG: 2005/09/07/1100–09/09/1221
2001-04-15%	1319	1350	1355	36	X14.4	S20W85	9415	B	350	13	8	6	50	6	6	–38	–36	–30	–114	–78	–34	
2003-10-29%	2037	2049	2101	24	X10.0	S15W02	10486	BGD	2,610	204	191	116	26	18	13	–350	–383	–307	–69	–41	–38	H/2054, *AS*/2,029, *SS*/2,628
1997-11-06%	1149	1155	1201	12	X9.4	S18W63	8100	BG	760	17	44	5	11	11	7	–34	–110	–35	–34	–54	–39	H/1211, *AS*/1,556, *SS*/1,604
2006-12-05%	1018	1035	1045	27	X9.0	S06E59	10930	B	390	3	26	25	24	8	16	–13	–55	–47	–36	–37	–37	LDG: 2006/12/04/0812–12/06/2012
2003-11-02%	1703	1725	1739	36	X8.3	S14W56	10486	BGD	2,160	18	13	38	6	17	8	–41	–38	–69	–41	–25	–20	H/1730, *AS*/2,598, *SS*/2,733
2005–01–20%	0636	0701	0726	50	X7.1	N14W61	10720	BGD	1,400	17	66	33	19	10	4	–53	–89	–97	–50	–39	–25	H/0654, *AS*/882, *SS*/951
2011-08-09	0748	0805	0808	20	X6.9	N17W69&	11263	BGD	340	8	6	4	4	4	9	–35	–25	–21	–22	–17	–18	H/0812, *AS*/1,610, *SS*/1,640
2006-12-06%	1829	1847	1900	31	X6.5	S05E57	10930	BGD	490	26	25	24	8	16	14	–55	–47	–36	–37	–37	–35	H/2012, *AS*/?, *SS*/?
2005-09-09%	1913	2004	2036	83	X6.2	S12E67	10808	BGD	1,430	17	33	101	75	44	18	–36	–73	–139	–89	–88	–69	H/1948, *AS*/2,257, *SS*/2,311
2001-12-13	1420	1430	1435	15	X6.2	N16E09	9733	BG	490	3	4	9	10	16	9	–39	–25	–11	–21	–39	–36	H/1454, *AS*/864, *SS*/1,315
2000-07-14%	1003	1024	1043	40	X5.7	N22W07	9077	BGD	460	51	164	50	8	12	14	–30	–289	–301	–114	–42	–36	H/1054, *AS*/1,674, *SS*/2,061
2001-04-06%	1910	1921	1931	21	X5.6	S21E31	9415	BG	860	13	20	63	20	11	85	–31	–42	–59	–63	–52	–271	H/1930, *AS*/1,270, *SS*/1,449
2012-03-07%	0002	0024	0040	38	X5.4	N17E27	11429	BGD	1,270	48	25	87	19	10	32	–85	–37	–143	–69	–46	–51	H/0024, *AS*/2,684, *SS*/3,146
2003-10-23%	0819	0835	0849	30	X5.4	S21E88	10486	BGD	1,160	6	38	16	10	11	25	–21	–44	–49	–33	–52	–32	
2005-09-08%	2052	2106	2117	25	X5.4	S12E75	10808	BG	510	6	17	33	101	75	44	–29	–36	–73	–139	–89	–88	LDG: 2005/09/07/1100–09/09/1221
2001-08-25	1623	1645	1704	41	X5.3	S17E34	9591	BGD	740	10	10	13	11	5	10	–1	–25	–13	–23	–13	–24	H/1650, *AS*/1,433, *SS*/1,629
2014-02-25	0039	0049	0103	24	X4.9	S12E82	11990	A	180	3	2	20	11	6	4	–22	–16	–99	–96	–50	–27	H/0126, *AS*/2,147, *SS*/?
1998-08-18	2210	2219	2228	18	X4.9	N33E87	8307	…	…	4	9	17	4	17	188	–11	–42	–67	–40	–43	–35	LDG: 1998/06/24/1155–10/15/1951
2002-07-23	0018	0035	0047	29	X4.8	S13E72	10039	BGD	940	17	7	12	12	17	11	–22	–21	–14	–21	–31	–18	H/0042, *AS*/2,285, *SS*/2,318
2000-11-26%	1634	1648	1656	22	X4.0	N18W38	9236	BG	600	28	45	31	56	6	6	–31	–80	–73	–119	–60	–44	H/1,706, *AS*/980, *SS*/1,094
			mean	35					943	25	41	40	28	20	21	–26	–38	–48	–41	–33	–27	
			sd	19					694	40	59	44	31	23	21	27	47	55	30	21	19	

Note: % means at least one disturbed day (Ap = 25+) follows the event during the interval elapsed time = 1–5 days
& means AR Loc comes from SOHO/LASCO Halo CME Catalog (http://cdaw.gsfc.nasa.gov/CME_list/halo/halo.html)
^ means AR data were taken from http://solarscience.msfc.nasa.gov/greenwch.shtml
Dur is the duration of the soft x-ray event from start to end
XRC is the x-ray class taken from http://www.ngdc.noaa.gov/stp/solar/solarflares.html
AR means Active Region
ARN means Active Region Number
ARMC means Active Region Magnetic Class
CARA means Corrected Active Region Area (in millionths of the solar hemisphere)
Ap is the planetary geomagnetic index in nT
Dst is the disturbance storm time index in nT
Ap and Dst available from http://omniweb.gsfc.nasa.gov/form/dx1.html
LDG means LASCO Data Gap
H means halo
AS means apparent speed in km per second
SS means space speed in km per second

Association	Equation	*r*	*rxr*	*se*	*cl*
SS vs. XRC	$y = 1{,}526.862 + 63.834x$	0.346	0.120	684.389	>99.5%
SS vs. Duration	$y = 1{,}324.933 + 9.609x$	0.429	0.184	658.967	>99.9%

								NXCE(x)						NXCE(HE)					NXCE(N-HE)					
Cycle	**<SSN>**	**NSXRE**	**NXCE**	**NHE**	**HE**	**N-HE**	**LDG**	**CD**	**NCD**	**U**	**<30**	**30–60**	**>60**	**CD**	**NCD**	**<30**	**30–60**	**>60**	**CD**	**NCD**	**U**	**<30**	**30–60**	**>60**
23	56.6	23,274	124	394	57	49	18	54	59	11	69	40	15	36	21	21	25	11	17	31	1	35	9	5
24#	39.4	10,114	42	247	23	19	0	16	21	5	23	11	8	8	15	12	6	5	11	7	1	11	4	4
Totals		33,388	166	641	80	68	18	70	80	16	92	51	23	44	36	33	31	16	28	38	2	46	13	9
23&		14,352	72	250	34	28	10	33	37	2	42	23	7	25	9	14	16	4	6	21	1	21	4	3

Note: # means the first 7 years of SC24 (2008–2014)
& means the first 7 years of SC23 (1996–2002)

Group	Duration			CMD		
	n	**mean**	***sd***	***n***	**mean**	***sd***
XCE(HE)	80	42	31	80	42	29
XCE(N-HE)	68	29	25	66	51	25
XCE(HE-G)	54	46	35	54	33	24
XCE(N-HE-G)	26	32	28	26	55	29
XCE(HE-NG)	26	34	21	26	60	29
XCE(N-HE-NG)	42	27	23	40	48	22